

# Cooperative Distributed Control Implementation of the Power Flow Coloring Over a Nano-Grid With Fluctuating Power Loads

Saher Javaid, Yuhei Kurose, Takekazu Kato, *Member, IEEE*, and Takashi Matsuyama

**Abstract**—To realize efficient and versatile energy management systems for future homes, buildings, and local communities, nano-grid (NG) finds possibility for integrating distributed energy resources. This paper implements the power flow coloring, which gives a unique ID to each power flow between a specific power source and a specific power load. It enables us to design versatile power flow patterns between distributed power sources and loads, taking into account energy availability, cost, and carbon dioxide emission. To implement the power flow coloring, this paper proposes a cooperative distributed control method, where a master–slave role assignment scheme of power sources and a time-slot based feedback control are introduced to cope with power fluctuations while keeping the voltage stability of the NG. Experimental results show the practical feasibility of our proposed method in managing distributed power sources and fluctuating loads.

**Index Terms**—Power flow coloring, cooperative distributed control, i-Energy, energy on demand, demand-side management.

## NOMENCLATURE

$P_{i,j}$	Nominal power supplied from $i$ th PS to $j$ th PL
$R_{i,j}$	PSR supplied from $i$ th PS to $j$ th PL
$P_{i,k}^s$	Average power supply by $SA_i$ in time-slot $k$
$P_{j,k}^l$	Average power consumption by $LA_j$ time-slot $k$
$T_{i,k}$	Target power level of $SA_i$ for time-slot $k$
$D_{i,k}$	Compensation factor for time-slot $k$
$\varepsilon_{j,k}^l$	Power consumption estimation error
$\varepsilon_{i,k}^s$	Power supply error
$L_{i,k}^s$	Power loss ascribed to $i$ th PS
$L_{j,k}^l$	Power loss ascribed to $j$ th PL
$D'_{i,k}$	Compensation factor with power loss
$T'_{i,k}$	Target power with power loss

## I. INTRODUCTION

IN RECENT years there has been growing interest in the demand side energy management. This is mainly because

residential and commercial buildings represent a major part of electricity consumptions and carbon dioxide emissions [1] and partly because small distributed power sources such as photovoltaics, wind turbines, fuel cells, and storage batteries have been introduced into houses, office buildings, and factories. The structure of residential and commercial areas will be changed drastically due to the deployment of such distributed power sources [2], [3].

One such energy management system is a Nano-grid (NG) [4]–[6]. It includes power generating sources, an in-house power distribution system, and energy storage functions as well as a variety of appliances such as lighting, TV, heating/ventilation/air conditioning, and cooking. NGs have been studied significantly for future power distribution architecture from tens of kW to MW leading to the micro-grid (MG) level [7], [8] and often operate over a simple shared power line.

Furthermore, a NG can operate independently or be connected to the national grid and can be designed for either AC or DC power management. Since a NG is usually connected to a MG or national grid, it has fewer issues in managing reactive power, frequency stability, and power loss. It is better to make a grid-connected NG to be able to operate in an off-grid mode optionally because it can cope with power failures in the national grid as well as can function even in developing countries without the national grid.

While a NG is a small compact grid system, it has to manage several power sources, storages, and a variety of appliances with diverse usage patterns taking into account energy availability, cost, and carbon dioxide emission. That is, a NG has to have a sophisticated control function of multiple power sources and storages so that they can cope with dynamically changing power consumption patterns and power supply conditions. We believe this is a new function to be developed for a NG.

In order to develop sophisticated systems with diverse components and versatile functions, it is a crucial and fundamental requirement to give a unique ID to each basic entity such as IP addresses in the Internet, social security numbers in welfare and health care systems etc. In [9] and [10], the concept of the *Power Flow Coloring* is proposed, which attaches the unique identification to each power flow between a pair of power source and load. While the concept of the power flow coloring can be applied to any types of grids, this paper focuses on the power flow coloring over NG. This is because the development of fundamental technologies for implementing the power

Manuscript received June 5, 2015; revised August 28, 2015 and November 9, 2015; accepted December 9, 2015. Date of publication January 25, 2016; date of current version December 21, 2016. Paper no. TSG-00620-2015.

The authors are with the Graduate School of Informatics, Kyoto University, Kyoto 6068501, Japan (e-mail: saherjavaid@i.kyoto-u.ac.jp; kurose@vision.kuee.kyoto-u.ac.jp; tkato@i.kyoto-u.ac.jp; tm@i.kyoto-u.ac.jp).

Color versions of one or more of the figures in this paper are available online at <http://ieeexplore.ieee.org>.

Digital Object Identifier 10.1109/TSG.2015.2509002

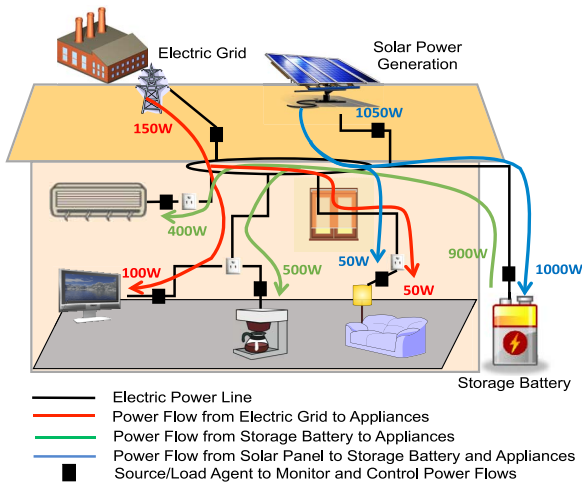


Fig. 1. The Power Flow Coloring.

flow coloring can be facilitated in a NG consisting of a shared bus power line without complicated power control devices for transmission and distribution. Fig. 1 illustrates the power flow coloring over a NG in a house. It enables us to design versatile power flow patterns between distributed power sources and loads. Note that as shown in Fig. 1, a power source can supply power flow streams to multiple loads and a load can be supplied power flow streams from multiple power sources. For example, watch a TV with the utility supplying power, use an air conditioner with photovoltaic power, make coffee using power stored in a battery, and mix 60% photovoltaic power and 40% battery power to operate a heater.

The power flow coloring can help in realizing the cost sensitive usage of power by evaluating power generation costs of power sources. The utilization of renewable energy sources to reduce atmospheric carbon dioxide would be another important motivation for the power flow coloring. Moreover, the power flow coloring can manage power flow streams with diverse characteristics. For example, the power generated by a photovoltaic is characterized by power fluctuations and available time periods. With the power flow coloring, a power with dynamic fluctuations can directly flow into a load which can accommodate the fluctuations such as heaters and coolers without affecting the other power flows. Consequently, we are able to use variety of power sources with diverse characteristics over the NG.

While some readers may recognize similarities between the popular consignment power supply and the power flow coloring, they differ in the following points:

**Real-Timeness:** Since the former manages volumes of power supply and consumption, real-time power control is not required. The latter, on the other hand, controls instantaneous power supply and consumption in real-time. More specifically, the system proposed in this paper uses three different time responses based on the control hierarchy: microscopic, mesoscopic, and macroscopic levels. The micro-level time response or hardware level uses 16.3 milliseconds control intervals to manage AC power and voltage [11]. The meso-level time response shows the communication interval of one-second

among distributed power sources and loads. The macro-level time response indicates operation mode changes of power loads by human, that can take several minutes or more.

**Stability Control:** Since the amount of power for the consignment power supply is far small compared to the base power managed, no additional control mechanism need to be introduced for the consignment power supply. In the latter case, however, since power flows to be managed over a NG are similar in their volumes, a sophisticated stability control mechanism should be developed at the same time as the power flow design. The system proposed in this paper employs a master-slave role assignment scheme to maintain the voltage stability of the NG against unexpected power fluctuations by power loads.

**Power Fluctuation Management:** Thanks to the real-time power control, the power flow coloring can manage dynamically fluctuating power sources and loads as described above, which is out of scope of the consignment power supply.

**Specification of Arbitrary Power Supply Mixture:** As described before, the power flow coloring can manage power flows from multiple power sources to one load. That is, a home user can specify how much power from which source is to be supplied for a particular power load taking into account energy availability, cost, and carbon dioxide emission.

This paper aims to implement the power flow coloring over a NG with fluctuating power loads while keeping the voltage stability of the NG. Note that with a power controllable load such as a heater, the proposed implementation method can be easily augmented to manage a fluctuating power source such as a photovoltaic.

The rest of the paper is organized as follows; Section II surveys related works and introduces our idea for the power flow coloring implementation. In Section III, we propose a cooperative distributed system architecture consisting of power managers, power source agents, and load agents. Section IV describes the basic message exchange protocol to implement the cooperative distributed control method. To cope with power fluctuations of loads as well as delays in message exchanges and computations, Section V introduces an augmented protocol with the master-slave role assignment for power source agents and the time-slot based feedback control. Following the practical protocol specification, its soundness proof and the management of power loss over a NG are described. In Section VI, the practicality of our implementation for the power flow coloring is demonstrated with experimental results. Section VII gives concluding remarks and future studies.

## II. MANAGING METHODS OF DISTRIBUTED POWER SOURCES AND IMPLEMENTATION METHODS OF THE POWER FLOW COLORING

With the advent of distributed power sources, a large number of new technologies of managing multiple power sources have been developed [12]–[16]. This is because characteristics of distributed power sources are very different from traditional power generators; the former includes DC power generation devices such as photovoltaics (PVs) and batteries while the latter generates AC power by mechanically rotating machines.

To integrate distributed power sources to the ordinary grid, a variety of power sharing schemes have been proposed [17], [18]. To achieve accurate power sharing while maintaining the voltage and frequency of a grid, there are two main types of control methods: centralized and decentralized. Centralized control based on a communication infrastructure [19], [20]. However, it is impractical to transmit dynamic data and control signal. The central controlling device should have the information of entire power network including (power sources and power loads). In order to overcome limitations of centralized control method, decentralized control methods are reported, which majorly applies droop control methods to integrate different power sources [5], [21], [22] for current sharing. This type of control does not need communication infrastructure, which actually helps in increasing the robustness of the entire system. However, the power sharing schemes just coordinate multiple power sources to supply the total power consumed by a group of power loads and hence cannot discriminate individual power consumptions of the power loads as in the power flow coloring.

To manage DC power sources, hybrid systems have also been proposed. Reference [23] proposed the optimal energy management system for hybrid power supply systems with PV and a battery, which uses power flow management to balance power streams between storage battery, PV panel and power load in grid-connected mode. In [24], on the other hand, optimal power flow management model is proposed for solar battery power supply system for off-grid application. The main objectives of these two systems are to satisfy the load power demand from PV power generation and minimize cost of fuel and battery system. These systems only consider the total power consumption as a whole for the power flow management therefore cannot distinguish individual power consumptions of the power loads.

On the other hand, power congestion problems are closely related or studied for the power transmission network management [25]–[27] in terms of capacity of grid. Congestion management ensures that the transmission flows remain within the transmission capacity. As NG is a small compact grid system consists of simple shared bus architecture, power congestion problem is out of scope of the NG.

Reference [28] proposed a theory of computing a detailed description of nodal prices in a grid: generation, transmission congestion, voltage limitation based on Kirchoff's laws and physical and economical constraints. While this theory enables us to compute the power flow on each individual power line connected to a power source or a load, an additional specification should be given to design which power sources supply powers to which power loads. Moreover, when the power consumption by a load fluctuates, a real-time controlling method of its power supplying sources should be developed.

While the concept of the power flow coloring shares some with above mentioned methods, its novelty rests in giving a unique ID to each individual power flow from a specific power source to a specific power load. Since it looks attractive, there have been proposed several implementation methods. They can be classified into three categories: power line switching, power routing, and synchronised source-load control.

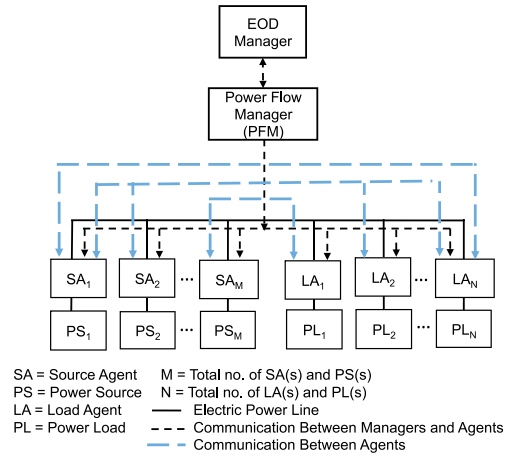


Fig. 2. System Architecture.

Okabe and Sakai [29] proposed a matrix power line switch between a group of power sources and a group of loads. By setting the switch, a physical power line connection is established between a power source and a load. While its control is simple, only one-to-one connection between a power source and a load can be realized and it cannot be scaled up without changing the existing grid.

Takuno *et al.* [30] and Abe *et al.* [31] proposed power routing methods. They developed so-called power routers which receive, store, and transmit chunks of power, power packets, just in the same way as message packet routers: a chunk of power is associated with source ID and destination ID. By introducing a multiplexing method, a simple power line can support multiple power packet transmissions. To realize this ID-based store-forward transmission, each power router should be equipped with a storage battery, which requires mass investments for the routing methods to be implemented in the existing grid. Moreover, since they focus on the power routing, no mechanism to control distributed power sources and loads is introduced.

The cooperative distributed control method for the power flow coloring proposed in this paper can be characterized by the synchronized source-load control method, one of whose advantages is that it can be used not only inside a household but also for local community in a NG without mass investments. Moreover, it manages power fluctuations of power sources and loads by controlling terminal devices real-time, which is the technical advantage of our proposed method. To implement the synchronized source-load control, we introduce a cooperative distributed system consisting of power managers, power source agents, and load agents, which communicate with each other to realize the power flow coloring while keeping the stability over the NG.

### III. SYSTEM ARCHITECTURE

In this section, a system architecture for the implementation of the power flow coloring over a NG is proposed (see Fig. 2). The proposed system is applied to a NG (e.g., in a household, building or local community), which consists of multiple power sources (PSs) and power loads (PLs) connected with



a common electric power line. A PS is an electric device which can supply electric power, e.g., solar panel, wind turbine and utility company. The PSs are considered with unique identifiers such as  $PS_i$  ( $i \in \{1, 2, \dots, M\}$ ) where  $M$  is the total no. of PSs. A set of PLs is also considered: a PL is an electric device that consumes electric power supplied by the PS(s). The proposed system comprises of  $N$  PLs with identifiers  $PL_j$  ( $j \in \{1, 2, \dots, N\}$ ). A power agent (i.e., source agent, SA or load agent, LA) is attached to each PS and PL, which measures and controls supply/consume power of the attached power device (PS/PL). All agents communicate with each other for the cooperative work to realize the power flow coloring. To specify, monitor, and maintain the overall power flow pattern, two types of power managers are introduced. The EoD manager conducts overall power management over the NG. It mediates all power demands required by loads based on the Energy on Demand Protocol and designs the overall power flow pattern (i.e., the power flow specification (PFS)) specifying which PS should supply how many Watts to which PL:

$$PFS = \begin{bmatrix} P_{11} & P_{12} & \dots & P_{1N} \\ P_{21} & P_{22} & \dots & P_{2N} \\ \vdots & \vdots & \ddots & \vdots \\ P_{M1} & P_{M2} & \dots & P_{MN} \end{bmatrix},$$

where,  $P_{MN}$  denotes the *nominal* power (in Watt) supplied from  $M$ th PS to  $N$ th PL. As for the EoD protocol see [32], [33]. Then, PFS is forwarded to the power flow manager (PFM), which monitors and coordinates SAs and LAs to maintain the specified PFS. As is well known, the power consumption by a load usually fluctuates and sometimes varies a lot due to automatic changes of its operation modes (e.g., automatic power control in an air conditioner). This means that the nominal power value specified in PFS is just a reference and hard to maintain physically. To bridge between this nominal and physical power values, PFM converts a given PFS into the power supply ratio (PSR) as follows:

$$PSR = [R_{ij}] = \left[ \frac{P_{ij}}{\sum_{i=1}^M P_{ij}} \right]$$

$$\sum_{i=1}^M R_{ij} = 1 \text{ for all } j,$$

where  $P_{ij}$  denotes the nominal power supplied from  $i$ th PS to  $j$ th PL and  $R_{ij}$  is PSR supplied from  $i$ th PS to  $j$ th PL. The PFM sends PSR to all SAs so that PSR is preserved against any power fluctuations by loads. Note that as will be described later, when the EoD manager wants to change PFS, it has to evaluate gaps between nominal and physical power supplies/consumptions based on the previous PFS and conduct some compensation process before designing a new PFS.

#### IV. BASIC SYSTEM PROTOCOL

This section describes the basic system protocol for the power flow coloring under an ideal situation. Here, it is

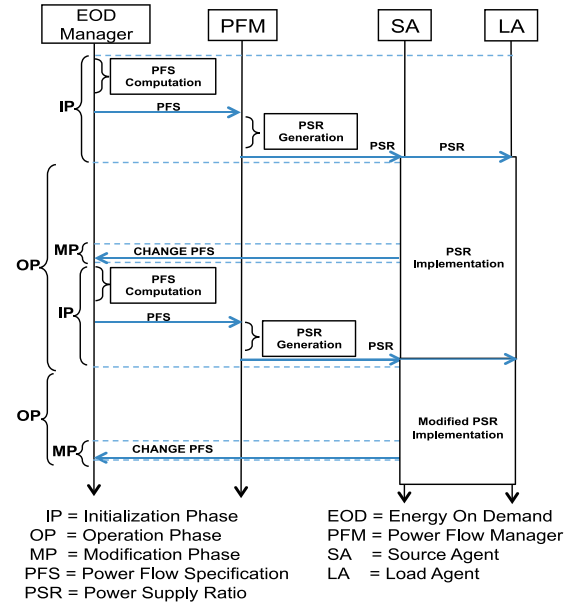


Fig. 3. Basic System Protocol.

assumed that all PSs and PLs are controllable, i.e., the power supply from PSs and power consumption by PLs can be controlled according to the specified PFS. We also assume that there is no power fluctuation, communication loss, communication delay, computation delay, control error, or power loss for the basic system protocol.

The protocol can be described by message exchanges among the managers and agents (Fig. 3). The protocol consists of three phases named as initialization phase (IP), operation phase (OP) and modification phase (MP). The EoD manager starts the IP by computing PFS and then sends it to PFM, which then compiles PFS to generate PSR. Finally, PSR is broadcasted to all SAs and LAs to maintain the specified power supply ratios during the OP. Thanks to the assumptions, no communication or control among the agents is required to maintain the specified PSR. The MP will start when any power agent observes an event that requires change in PFS. The event could be any change in user behaviors (e.g., want to see TV), in power consumption (e.g., a heater is switched ON/OFF by a thermostat), or in power supply (e.g., a utility company issues a Demand Response signal to suppress power usage). After observing such event, the agent sends a CHANGE PFS message to the EoD manager, which then designs a new PFS to cope with the reported event and forwards it to PFM. Finally a new OP is started by PFM. While the above process is enough for the basic system protocol, a practical protocol should include an additional process in the MP to compensate the gap between the nominal and physical power. That is, to design a new PFS, the EoD manager first collects physically supplied/consumed powers from SAs and LAs and computes differences from the nominal powers specified by PFS. How to compensate the differences in the new PFS should be decided based on technical and economic policies for the EoD manager to comply with.

## V. AUGMENTED SYSTEM PROTOCOL

The basic system protocol relies on many assumptions and hence should be augmented to implement the power flow coloring in the real world. This section describes an augmented system protocol for the real world scenario.

To deal with practical situations, there is a need to manage power fluctuations of power devices. Here power fluctuations include both noisy fluctuations and power variations. Noisy fluctuations are physical power fluctuations due to the nature of power sources and loads. On the other hand, power variations are caused by operation mode changes of PSs/PLs (e.g., ON/OFF status changes, low power to/from high power supply/consumption etc.) The augmented system protocol proposed in this paper is designed to manage real-time power fluctuations of PLs alone. To implement such management, a time-slot based feedback control method is introduced into the basic system protocol: it maintains the specified PSR even if consumed powers by PLs fluctuate unexpectedly due to noise and vary a lot by their operation mode changes. How to manage power fluctuations of PSs is reserved for future studies.

Even if power fluctuations are confined to those by PLs, the power fluctuation management leads us to another augmentation. That is, there is a need to introduce a mechanism to maintain the voltage stability of the NG against physical power fluctuations. For this purpose, the master and slave role assignment scheme is introduced among SAs: one SA is selected as a master and maintains the voltage stability of the NG against power fluctuations caused by PLs. The third augmentation is required to cope with communication and computation delays by SAs and LAs. This is also essential in real world systems for power management because electrical devices operate continuously without any break. As will be described later, the time-slot based feedback control method can be designed to hide communication and computation delays in a systematic way.

In summary, the augmented system protocol should satisfy at least the following three requirements to work in the real world:

- Maintain the voltage stability of the NG,
- Maintain the specified PSR against power fluctuation (both noisy fluctuations and power variations), and
- Cope with communication and computation delays.

### A. Master and Slave Architecture

Unexpected power fluctuations caused by PLs easily make the NG unstable leading to blackouts. To maintain the voltage stability of the NG against power fluctuations, the master and slave role assignment scheme has been proposed among SAs. One of the SAs is selected as the master that operates as voltage and phase sources. Master SA supplies and absorbs any amount of active power (fluctuation) to maintain the voltage level of the NG. The internal power control device as well as its corresponding PS of the master SA should be equipped with enough physical functions and power supply capacity to fulfil the role of the master. A utility power line or a large-scale storage battery is a candidate of the master SA.

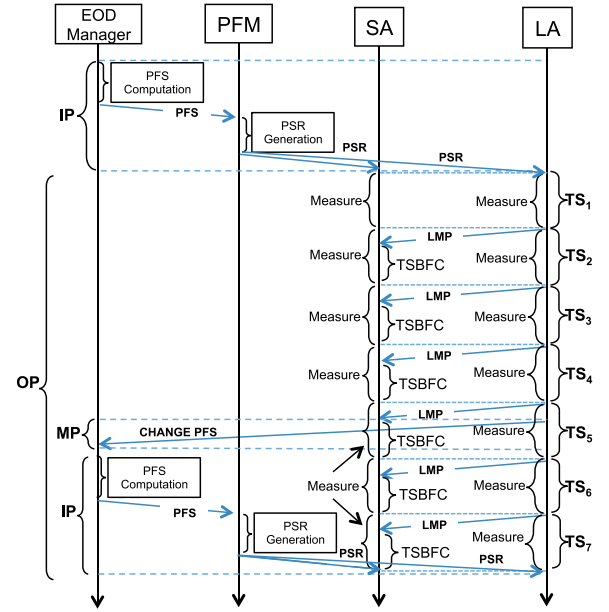


Fig. 4. Augmented System Protocol.

Note that while the current implementation is designed for an AC power NG, it manages the active power alone and is to be augmented further to manage the reactive power.

All SAs except the master operate as slaves. They work as active power sources and supply specified powers without caring about any power fluctuations. That is, the internal power device and its corresponding PS of each slave SA keep supplying the specified power level by its internal local feedback control. How to compute and modify the power specification for each slave SA based on the given PSR will be described later. As for physical implementation of master and slave, refer to Section VI.

Note that while the master SA does not care about its specified power supply, the specified PSR can be maintained completely, which will be discussed later too. Note also that when the NG includes multiple PSs enough capable to work as the master SA, the role of the master can be switched dynamically based on the NG management policy.

### B. Time-Slot Based Feedback Control (TSBFC) Method

Since the voltage stability is maintained by the master SA, it is necessary to develop a method to solve the remaining two problems: cope with unexpected power fluctuations of PLs while keeping the specified PSR and make the power management operate continuously without being affected by communication and computation delays. Hence, TSBFC is developed to solve these problems in a systematic way. Note that TSBFC is conducted by all slave SAs and no explicit power control to comply with the specified PSR is conducted by the master SA.

1) *Time-Slot and Protocol Description:* First, the time axis is partitioned into a series of time-slots (TSs) with a fixed length and the operation phase is represented by a series of TS<sub>k</sub> ( $k = 1, 2, \dots$ ) (Fig. 4). While in what

follows it is assumed that all SAs and LAs share the common time axis, the augmented system protocol accommodates small discrepancies among local clocks in SAs and LAs. That is, SAs and LAs can run asynchronously based on their internal clocks without exchanging any synchronization messages.

At the very beginning, the first initialization phase is conducted by the EoD manager and PFM. Then PFM broadcasts the PSR to all SAs and LAs to start the operation phase. The first TS of the operation phase is TS<sub>1</sub>. During TS<sub>1</sub>, all LAs and SAs just measure power consumptions by their corresponding PLs and power supplies by their corresponding PSs respectively. That is, no power control is conducted in TS<sub>1</sub>. Note that as will be described later in this section, since TSBFC can cope with large power variations (i.e., switching a PL ON/OFF) keeping the specified PSR, it is assumed that all PLs are OFF at the beginning of the operation phase and switched ON later in the operation phase.

In TS<sub>2</sub>, each LA sends the average power consumption value (Watt) in TS<sub>1</sub> to all SAs that supply powers to that LA, while keeping the power consumption measurement in TS<sub>2</sub>. This message transmission is shown as *load measured power (LMP)* message in Fig. 4. When each SA receives the average power consumption data in TS<sub>1</sub> from its corresponding LAs, it calculates the target power level to supply for the next TS (i.e., TS<sub>3</sub>) while keeping the power supply measurement in TS<sub>2</sub>. The target power level computation algorithm will be described later. Note that no power control is conducted in TS<sub>2</sub> either.

In TS<sub>k</sub>  $k \geq 3$ , each LA measures its power consumption during TS<sub>k</sub> and in TS<sub>k+1</sub> reports it to all SAs that supply powers to it. Each SA (except the master SA), on the other hand, collects power consumption data in TS<sub>k-2</sub> from all LAs which are supplied power from that SA and computes the target power level to supply in TS<sub>k</sub>. These message receipt and computation are conducted during TS<sub>k-1</sub> while the power supply according to the target power level for TS<sub>k-1</sub> as well as the power supply measurement in TS<sub>k-1</sub> are being continued. With these overlaid executions of communication and computation with measurement and control, TSBFC can realize the continuous power flow coloring in the real world.

2) *Feedback Control Method*: Here, the algorithm for each slave SA is addressed to compute the target power level for TS<sub>k</sub>  $k \geq 3$ , which realizes the feedback control to maintain the specified PSR against unexpected power fluctuation. Note that the algorithm processes average power consumption and supply levels in TS<sub>k</sub> instead of instantaneous power levels. Let  $P_{j,k}^l$  denotes the average power consumption by LA<sub>j</sub> in TS<sub>k</sub> and  $P_{i,k}^s$  is the average power supply by SA<sub>i</sub> in TS<sub>k</sub>. As described above, the target power level ( $T_{i,k}$ ) of SA<sub>i</sub> for the next time-slot TS<sub>k</sub> is calculated based on the power consumption and supply data measured in TS<sub>k-2</sub>. This computation is done during TS<sub>k-1</sub>.

To implement the feedback control, there is a need to evaluate the difference between the actual power supply by SA<sub>i</sub> in TS<sub>k-2</sub>,  $P_{i,k-2}^s$ , and the actually consumed powers in TS<sub>k-2</sub> by such LAs that received power from SA<sub>i</sub>. Then, this difference should be compensated in TS<sub>k</sub>. So this difference is denoted

as  $D_{i,k}$  meaning the compensation factor for TS<sub>k</sub>, which is defined as follows:

$$D_{i,k} = \sum_{j=1}^N R_{ij} \cdot P_{j,k-2}^l + D_{i,k-2} - P_{i,k-2}^s \quad (1)$$

where  $R_{ij}$  denotes the PSR specified for SA<sub>i</sub> by PFM. Note that for all slave SA<sub>i</sub>,  $D_{i,0} = D_{i,1} = 0$  because no power control is conducted in TS<sub>0</sub> or TS<sub>1</sub> as described before.

Then, the target power level ( $T_{i,k}$ ) of SA<sub>i</sub> for the next time-slot TS<sub>k</sub> is defined as,

$$T_{i,k} = \sum_{j=1}^N R_{ij} \cdot P_{j,k-2}^l + D_{i,k} \quad (2)$$

Here again  $T_{i,1} = T_{i,2} = 0$  since no power control is conducted in TS<sub>1</sub> and TS<sub>2</sub>. In this definition, it is assumed that all LAs will consume the same amount of power in TS<sub>k</sub> as that measured in TS<sub>k-2</sub>. To implement a more sophisticated feedback control,  $P_{j,k-2}^l$  should be replaced with the predicted power consumption by LA<sub>j</sub> in TS<sub>k</sub>,  $\hat{P}_{j,k}^l$ .

As noted before, when the PFS is modified and a new operation phase is to be started from TS<sub>k</sub>, some inter operation phase compensation process should be conducted using  $D_{i,k}$  and  $D_{i,k+1}$  in the new operation phase, which is reserved for future study.

### C. Soundness Proof of the Augmented Protocol

The soundness of the augmented system protocol can be proved by convergence of TSBFC and Preservation of PSR. For this proof, it is assumed that each PL is switched OFF at the beginning (i.e.,  $k = 1$ ), operate for sometime, will be switched OFF again (i.e.,  $k = K$ ), and keeps OFF until  $k = T$  ( $T$ : the last time slot index under consideration). Under this assumption, it can be proved easily that  $D_{i,k}$  is not accumulated and converges to 0 and that the specified PSR is attained without being affected by power fluctuations of PLs.

1) *Convergence of TSBFC*: Here, two types of errors are considered; the power consumption estimation error and power supply error. Due to the power fluctuation of each PL, the power consumption estimation error can occur which can be represented as follows since the current TSBFC employs  $P_{j,k-2}^l$  as the estimated power consumption for the time slot  $k$ .

$$\varepsilon_{j,k}^l = P_{j,k}^l - P_{j,k-2}^l \quad (3)$$

On the other hand, due to physical device characteristics of each PS, the power supply error can be experienced that can be defined as,

$$\varepsilon_{i,k}^s = P_{i,k}^s - T_{i,k} \quad (4)$$

By considering these two errors, the compensation factor described in equation (1) can be written as,

$$D_{i,k} = \sum_{j=1}^N R_{ij} (P_{j,k-4}^l + \varepsilon_{j,k-2}^l) + D_{i,k-2} - (T_{i,k-2} + \varepsilon_{i,k-2}^s)$$

By using equation (2),

$$\begin{aligned}
&= \sum_{j=1}^N R_{ij} (P_{j,k-4}^l + \varepsilon_{j,k-2}^l) + D_{i,k-2} \\
&\quad - \left( \sum_{j=1}^N R_{ij} \cdot P_{j,k-4}^l + D_{i,k-2} + \varepsilon_{i,k-2}^s \right) \\
&= \sum_{j=1}^N R_{ij} \cdot P_{j,k-4}^l + \sum_{j=1}^N R_{ij} \cdot \varepsilon_{j,k-2}^l + D_{i,k-2} \\
&\quad - \left( \sum_{j=1}^N R_{ij} \cdot P_{j,k-4}^l - D_{i,k-2} - \varepsilon_{i,k-2}^s \right) \\
&= \sum_{j=1}^N R_{ij} \cdot \varepsilon_{j,k-2}^l - \varepsilon_{i,k-2}^s
\end{aligned}$$

Under the given assumption, for any  $T \geq k \gg K$ ,  $\varepsilon_{j,k-2}^l - \varepsilon_{i,k-2}^s = 0$  and  $D_{i,k} = 0$  which clearly shows that the errors are not accumulated and TSBFC converges at  $T$ .

2) *Preservation of PSR*: This section shows that the preservation of PSR is maintained appropriately throughout the NG including Slave PSs and Master PS. At first, the PSR preservation by a slave PS is proved. If the PSR for  $i$ th slave PS is maintained in the period between the first TS ( $k = 1$ ) to the last TS ( $k = T$ ), then the following equation should hold.

$$\sum_{k=1}^T \left( P_{i,k}^s - \sum_{j=1}^N R_{ij} \cdot P_{j,k}^l \right) = 0 \quad (5)$$

To prove this equation (5), the left hand side can be written as follows using equations (3) and (4).

$$= \sum_{k=1}^T \left( T_{i,k} + \varepsilon_{i,k}^s - \sum_{j=1}^N R_{ij} (P_{j,k-2}^l + \varepsilon_{j,k}^l) \right)$$

By using equation (2),

$$\begin{aligned}
&= \sum_{k=1}^T \left( \sum_{j=1}^N R_{ij} \cdot P_{j,k-2}^l + D_{i,k} + \varepsilon_{i,k}^s - \sum_{j=1}^N R_{ij} (P_{j,k-2}^l + \varepsilon_{j,k}^l) \right) \\
&= \sum_{k=1}^T \left( D_{i,k} + \varepsilon_{i,k}^s - \sum_{j=1}^N R_{ij} \cdot \varepsilon_{j,k}^l \right)
\end{aligned}$$

By using the result of convergence of TSBFC,

$$\begin{aligned}
&= \sum_{k=1}^T \sum_{j=1}^N R_{ij} \cdot \varepsilon_{j,k-2}^l - \sum_{k=1}^T \varepsilon_{i,k-2}^s + \sum_{k=1}^T \varepsilon_{i,k}^s \\
&\quad - \sum_{k=1}^T \sum_{j=1}^N R_{ij} \cdot \varepsilon_{j,k}^l \\
&= \sum_{k=1}^{T-2} \sum_{j=1}^N R_{ij} \cdot \varepsilon_{j,k}^l - \sum_{k=1}^{T-2} \varepsilon_{i,k}^s + \sum_{k=1}^{T-2} \varepsilon_{i,k}^s + \varepsilon_{i,T-1}^s + \varepsilon_{i,T}^s \\
&\quad - \sum_{k=1}^{T-2} \sum_{j=1}^N R_{ij} \cdot \varepsilon_{j,k}^l - \sum_{j=1}^N R_{ij} \cdot \varepsilon_{j,T-1}^l - \sum_{j=1}^N R_{ij} \cdot \varepsilon_{j,T}^l \\
&= \varepsilon_{i,T-1}^s + \varepsilon_{i,T}^s - \sum_{j=1}^N R_{ij} \cdot \varepsilon_{j,T-1}^l - \sum_{j=1}^N R_{ij} \cdot \varepsilon_{j,T}^l
\end{aligned}$$

Then under the given assumption, for any  $T \geq k \gg K$ ,  $\varepsilon_{i,T-1}^s = \varepsilon_{i,T}^s = \varepsilon_{j,T-1}^l = \varepsilon_{j,T}^l = 0$ , which proves equation (5) holds. For master PS, the total supply power can be written as,

$$P_{m,k}^s = \sum_{j=1}^N P_{j,k}^l - \sum_{i=1, i \neq m}^M P_{i,k}^s, \quad (6)$$

where  $m$  indicates master PS. Then, if the PSR for the master PS is maintained in the period between the first TS ( $k = 1$ ) to the last TS ( $k = T$ ), the following equation should hold.

$$\sum_{k=1}^T \left( P_{m,k}^s - \sum_{j=1}^N R_{mj} \cdot P_{j,k}^l \right) = 0 \quad (7)$$

The left hand side can be written as follows by using equation (6) and the definition of PSR,

$$\begin{aligned}
&= \sum_{k=1}^T \left( \sum_{j=1}^N P_{j,k}^l - \sum_{i=1, i \neq m}^M P_{i,k}^s - \sum_{j=1}^N \left( 1 - \sum_{i=1, i \neq m}^M R_{ij} \right) P_{j,k}^l \right) \\
&= \sum_{k=1}^T \left( \sum_{j=1}^N P_{j,k}^l - \sum_{i=1, i \neq m}^M P_{i,k}^s - \sum_{j=1}^N P_{j,k}^l \right. \\
&\quad \left. + \sum_{j=1}^N \sum_{i=1, i \neq m}^M R_{ij} \cdot P_{j,k}^l \right) \\
&= \sum_{i=1, i \neq m}^M \sum_{k=1}^T \left( P_{i,k}^s - \sum_{j=1}^N R_{ij} \cdot P_{j,k}^l \right)
\end{aligned}$$

From the PSR preservation of a slave PS, this term can be represented as follows.

$$= - \sum_{i=1, i \neq m}^M \left( \varepsilon_{i,T-1}^s + \varepsilon_{i,T}^s - \sum_{j=1}^N R_{ij} \cdot \varepsilon_{j,T-1}^l - \sum_{j=1}^N R_{ij} \cdot \varepsilon_{j,T}^l \right)$$

Then under the given assumption, for any  $T \geq k \gg K$ ,  $\varepsilon_{i,T-1}^s = \varepsilon_{i,T}^s = \varepsilon_{j,T-1}^l = \varepsilon_{j,T}^l = 0$ , which proves equation (7) holds.

While it is proved that equation (5) holds for each PS, the equation means just the necessary condition for the PSR preservation. That is, another PSR different from  $R_{ij}$ , say  $Q_{ij}$ , may satisfy equation (5). To put this in another way, given observed power supply data,  $\sum_{k=1}^T P_{i,k}^s (i = 1, \dots, M)$ , and observed power consumption data,  $\sum_{k=1}^T P_{j,k}^l (j = 1, \dots, N)$ , equation (5) may have multiple solutions, each of which gives a different power flow pattern. The important point here is that the specified PSR is one of such solutions and hence it is sound that power flow streams from PSs to PLs can be interpreted as being distributed according to the specified PSR.

#### D. Managing Power Loss Over a NG

So far it is assumed that no power is lost during power transmission from PSs to PLs. In this section, introduction of a power loss management method is proposed into the augmented protocol described before.

In practical situations, the total sum of the supplied power flow streams does not coincide with the total sum of the consumed power flow streams due to the power loss over a power



transmission inside NG. The difference between these two can be regarded as the total power loss. Then the accumulated power loss in the  $TS_k$  can be defined as,

$$L_k = \sum_{j=1}^M P_{i,k}^s - \sum_{i=1}^N P_{j,k}^l \quad (8)$$

Note that even without any power loss management, this accumulated power loss is supplied by the Master PS thanks to the stability maintenance mechanism by the master-slave architecture described before. However, to realize a fair usage of PSs it is better to introduce a power loss management method.

Since power losses are introduced by electrical lines connected to both PSs and PLs, the accumulated power loss can be decomposed as follows.

Power loss ascribed to  $PS_i$ :

$$L_{i,k}^s = \frac{P_{i,k}^s}{\sum_{i=1}^M P_{i,k}^s + \sum_{j=1}^N P_{j,k}^l} \cdot L_k \quad (9)$$

Power loss ascribed to  $PL_j$ :

$$L_{j,k}^l = \frac{P_{j,k}^l}{\sum_{i=1}^M P_{i,k}^s + \sum_{j=1}^N P_{j,k}^l} \cdot L_k \quad (10)$$

To realize a fair power supply among master and slave PSs, each slave PS should supply additional power to compensate power losses to which that PS is responsible. To this end, the following new compensation factor is introduced into TSBFC:

$$D'_{i,k} = L_{i,k-2}^s + \sum_{j=1}^N R_{ij} \cdot L_{j,k-2}^l \quad (11)$$

Then, the target power supply for  $PS_i$  in  $TS_k$  is defined as follows.

$$T'_{i,k} = \sum_{j=1}^N R_{ij} \cdot P_{j,k-2}^l + D_{i,k} + D'_{i,k} \quad (12)$$

This section introduced a new feature to the augmented protocol to realize the fair power loss management.

Note that the power flow coloring can be implemented not only in one household but also among many households, offices, and factories. In the latter case, the question arises who should pay for power losses. This economical aspect of the power flow coloring can be designed based on equations (9) and (10).

## VI. EXPERIMENTAL RESULTS

To show that the proposed system works in real physical environments satisfying three main requirements described in Section V, (i) maintain stability, (ii) keep PSR (power supply ratio) against power fluctuations of LAs, and (iii) accommodate communication and computation delays, at first a power distributor module is developed. It consists of a bi-directional AC-DC converter, a microprocessor, and a ZigBee wireless communication device. The real-time (i.e., 16.3 msec control interval) PWM control is conducted to make it work both as a voltage source (i.e., as a master power source) and as a power source (i.e., as a slave power source). Moreover, the frequency

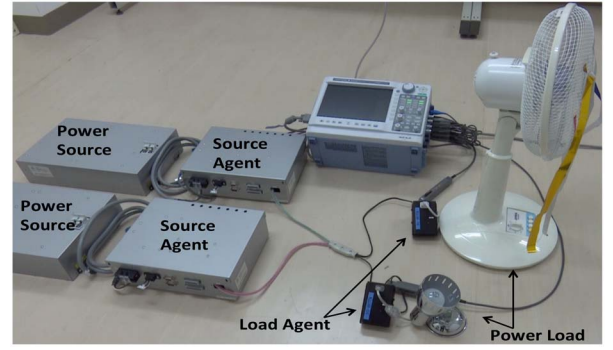


Fig. 5. Physical Environment Setup.

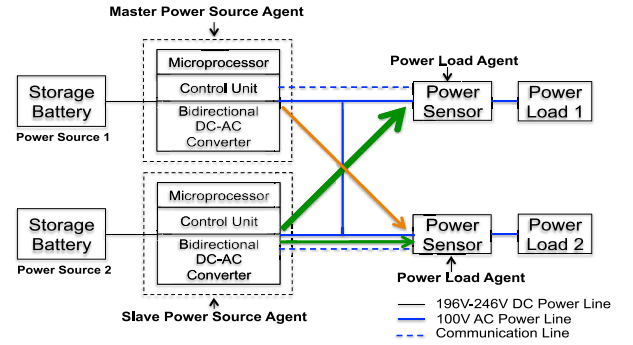


Fig. 6. Experimental Setup.

and phase control can be done both in a grid-connected mode and in a grid-off mode. As for technical details of the power distributor module, please refer to [11].

Figs. 5 and 6 illustrate physical and experimental settings for a grid-off mode operation of our system, where a pair of DC V power storage batteries are used as independent power sources. Each battery is connected to a common AC 100V power line via a power distributor. On the other hand, two loads are connected to the common AC 100V power line via smart taps [10], power sensors with embedded microprocessors and ZigBee wireless communication devices, respectively. On these hardware devices, we implemented the augmented system protocol described in Section V: a pair of power source agents supply power to a pair of load agents.

As shown in Fig. 5, an oscilloscope is used to measure detailed fluctuations of power supply and consumption. Moreover, in the following experiments, a pair of programmable power load devices were used instead of ordinary appliances. This is because accurately programmed fluctuations of power consumptions are useful to analyze detailed dynamical characteristics of the proposed system.

While couple of experiments under a variety of conditions are conducted, the following result shows a typical characteristic of the proposed system. PSR and the master-slave assignment are specified manually. That is the experimental setup does not include the EoD manager or PFM. The  $PS_1$  acts as master SA and  $PS_2$  acts as slave SA.  $SA_1$  supplies 50% power to  $LA_2$  while  $SA_2$  supplies 100% power to  $LA_1$  and 50% power to  $LA_2$ . Then PSR can be represented as,

$$PSR = \begin{bmatrix} 0 & 0.5 \\ 1.0 & 0.5 \end{bmatrix}$$



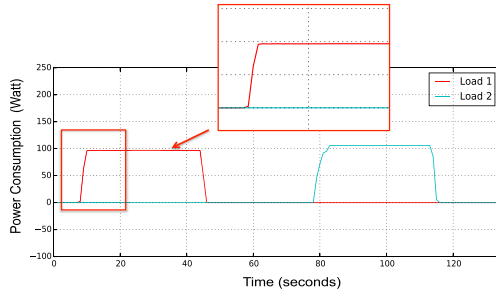


Fig. 7. Power Consumption by PLs (PL<sub>1</sub> and PL<sub>2</sub>).

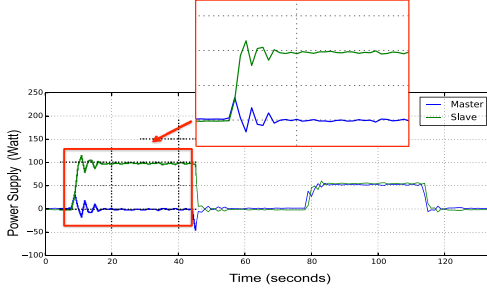


Fig. 8. Power Supply from PSs (Master and slave).

It means the supply power should be  $PS_1 = 0.5PL_2$  and  $PS_2 = PL_1 + 0.5PL_2$  respectively. The duration of time slot for TSBFC is set to  $TS = 1\text{sec}$ . At the starting time of the experiment, both PL<sub>1</sub> and PL<sub>2</sub> are switched OFF. Then as illustrated in Fig. 7, PL<sub>1</sub> (red line in Fig. 7) is switched ON, continues working for a while, and then switched OFF manually. PL<sub>2</sub> (green line in Fig. 7), on the other hand, is switched ON after PL<sub>1</sub> is switched OFF.

Fig. 8 illustrates dynamic profiles of power supplies by SAs. When PL<sub>1</sub> is switched ON, slave SA (i.e., SA<sub>2</sub>, green line in Fig. 8) supplies 100% power to PL<sub>1</sub> as specified in PSR. Since the power consumption by PL<sub>1</sub> changes largely, the power supply by SA<sub>2</sub> oscillates for several time slots as illustrated in the closed-up graph in Fig. 8. This oscillation is introduced by TSBFC conducted by SA<sub>2</sub>. Then master SA, SA<sub>1</sub> automatically stabilizes (absorbs) the oscillation by maintaining the voltage level of the NG as shown by the blue line in the closed-up graph in Fig. 8 and hence no oscillation is observed in the power consumption by PL<sub>1</sub> as shown by the red line in the closed-up graph in Fig. 7.

That is, the electric bulb of PL<sub>1</sub> does not cause any flickering. The same stabilization effects by master SA can be observed when PL<sub>1</sub> and PL<sub>2</sub> are switched ON or OFF in Figs. 7 and 8. When PL<sub>2</sub> is switched ON, both SA<sub>1</sub> and SA<sub>2</sub> supply 50% power respectively following the specified PSR. Figs. 7 and 8 prove that the power supply to a specific load from multiple power sources can be realized stably, i.e., no power oscillation is observed as shown by the green line in Fig. 7 and PSR is maintained, i.e., both SA<sub>1</sub> and SA<sub>2</sub> supply 50% power as shown by overlapping blue and green lines in the right part of Fig. 8.

Fig. 9 shows the accumulated power supplies by Master (PS<sub>1</sub>) and Slave (PS<sub>2</sub>) (solid lines) and corresponding

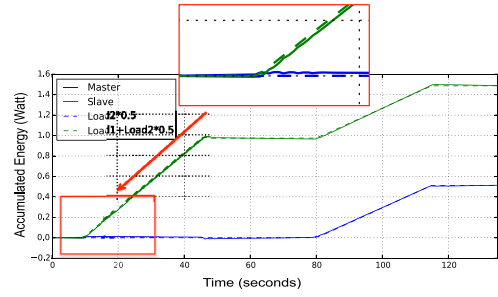


Fig. 9. Accumulated power supplies and consumptions of PSs and PLs.

accumulated power consumptions:  $0.5PL_2$  (blue dotted line) and  $PL_1 + 0.5PL_2$  (green dotted line). We can see that the specified PSR is maintained accurately against large power variations caused by unexpected power ON/OFF of PLs. This also demonstrates that TSBFC works continuously without accumulating errors and being affected by communication and computation delays.

Finally, we measured fluctuations of the effective voltage at the shared power bus during the experiment to show the effectiveness of our voltage stability control by the master SA working as the voltage source. We obtained the following statistical measures: number of measured samples: 29,140, average: 100.106V, max: 100.810V, min: 98.813V, and standard deviation: 0.123V. The reason why the average was slightly off the target value of the voltage stability control, i.e., 100V, is that the internal voltage sensor of the power distributor was not so accurately calibrated as the measuring instrument. These measures verified that the voltage of the power bus line is maintained stably.

## VII. CONCLUSION

This paper proposed a cooperative distributed control method to implement the power flow coloring over a NG with distributed power sources and fluctuating loads while keeping the voltage stability of the NG. The power flow coloring gives a unique ID to each individual power flow from a specific power source to a specific power load. It enables us to design versatile power flow patterns between multiple power sources and loads. Following the protocol specification, its soundness is proved and discussed the management of power loss over a NG.

To make proposed method work in real living environments, the following augmentations to solve physical, communicational, and computational problems should be implemented: (1) how to manage reactive power, (2) a more sophisticated feedback control method is required i) to suppress power supply oscillations when power consumptions by loads vary rapidly, ii) to cope with noise and uncertain data, and iii) to improve the resilience against message losses and malfunctions of devices, (3) an inter operation phase compensation process should be developed for a long run operation including changes of PFSs, (4) how to change role assignments among master and slave SAs while keeping stable power supplies to all power loads, (5) the currently implemented EoD system [32], [33] should be augmented to be able to

design PFS based on power requests from loads, (6) how to scale-up proposed method to realize the power flow coloring over a national grid including transmission and distribution network with loops, and finally (7) how to manage fluctuating and uncontrollable power sources like PVs. Some of these problems have been solved, which will be reported in a new paper.

## REFERENCES

- [1] M. Biabani, M. A. Golkar, A. Johar, and M. Johar, "Propose a home demand-side-management algorithm for smart nano-grid," in *Proc. 4th Power Electron. Drive Syst. Tech. Conf. (PEDSTC)*, Tehran, Iran, 2013, pp. 487–494.
- [2] B. Asare-Bediako, W. L. Kling, and P. F. Robeiro, "Home energy management systems: Evolution, trends and frameworks," in *Proc. IEEE 47th Int. Univ. Power Eng. Conf. (UPEC)*, London, U.K., 2012, pp. 1–5.
- [3] M. H. Shwehdi and S. R. Muhammad, "Proposed smart DC nano-grid for green buildings—A reflective view," in *Proc. Int. Conf. Renew. Energy Res. Appl. (ICRERA)*, Milwaukee, WI, USA, 2014, pp. 765–769.
- [4] M. C. Kinn, "Proposed components for the design of a smart nano-grid for a domestic electrical system that operates at below 50V DC," in *Proc. IEEE PES Int. Conf. Exhibit. Innov. Smart Grid Tech. (ISGT Europe)*, Manchester, U.K., 2011, pp. 1–7.
- [5] J. Schonberger, R. Duke, and S. D. Round, "DC-bus signaling: A distributed control strategy for a hybrid renewable nano-grid," *IEEE Trans. Ind. Electron.*, vol. 53, no. 5, pp. 1453–1460, Oct. 2006.
- [6] S. H. Latha and S. C. Mohan, "Centralized power control strategy for 25 kW nano grid for rustic electrification," in *Proc. IEEE Int. Conf. Emerg. Trends Sci. Eng. Tech. (INCOSSET)*, Tiruchirappalli, India, 2012, pp. 456–461.
- [7] W. Zhang, F. C. Lee, and P.-Y. Huang, "Energy management system control and experiment for future home," in *Proc. IEEE Energy Convers. Congr. Expo. (ECCE)*, Pittsburgh, PA, USA, 2014, pp. 3317–3324.
- [8] N. Hatziaargyriou, H. Asano, R. Iravani, and C. Marnay, "Microgrids," *IEEE Power Energy Mag.*, vol. 5, no. 4, pp. 78–94, Jul./Aug. 2007.
- [9] T. Matsuyama, "Creating safe, secure, and environment-friendly lifestyles through i-Energy," *New Breeze*, vol. 21, no. 2, pp. 1–8, 2009.
- [10] T. Matsuyama, "i-Energy: Smart demand-side energy management," in *Smart Grid Applications and Developments*. Berlin, Germany: Springer-Verlag, ch. 8, 2014.
- [11] T. Edagawa, K. Fukae, and T. Hisakado, "Peer-to peer energy transmission system by bidirectional AC-DC converter module," *Inst. Elect. Eng. Japan, Tech. Rep. PE-14-191, PSE-14-191*, 2014.
- [12] J. Han, C.-S. Choi, W.-K. Park, I. Lee, and S.-H. Kim, "Smart home energy management system including renewable energy based on ZigBee and PLC," *IEEE Trans. Consum. Electron.*, vol. 60, no. 2, pp. 198–202, May 2014.
- [13] J. Han, C.-S. Choi, W.-K. Park, I. Lee, and S.-H. Kim, "PLC-based photovoltaic system management for smart home energy management system," *IEEE Trans. Consum. Electron.*, vol. 60, no. 2, pp. 184–189, May 2014.
- [14] I. Hong, B. Kang, and S. Park, "Design and implementation of intelligent energy distribution management with photovoltaic system," *IEEE Trans. Consum. Electron.*, vol. 58, no. 2, pp. 340–346, May 2012.
- [15] Y. Rashidi, M. Moallem, and S. Vojdani, "Wireless ZigBee system for performance monitoring of photovoltaic panels," in *Proc. IEEE Photovolt. Spec. Conf.*, Seattle, WA, USA, 2011, pp. 3205–3207.
- [16] X. Xiaoli and Q. Daoe, "Remote monitoring and control of photovoltaic system using wireless sensor network," in *Proc. Int. Conf. Elect. Inf. Control Eng.*, Wuhan, China, 2011, pp. 633–638.
- [17] Y. A.-R. I. Mohammad and E. F. El-Saadany, "Adaptive decentralised droop controller to preserve power sharing stability of paralleled inverters in distributed generation micro grids," *IEEE Trans. Power Electron.*, vol. 23, no. 6, pp. 2806–2816, Nov. 2008.
- [18] L.-Y. Lu and C.-C. Chu, "Autonomous power management and load sharing in isolated micro-grids by consensus-based droop control of power converters," in *Proc. 1st Int. Conf. Future Energy Electron.*, Tainan, Taiwan, 2013, pp. 365–370.
- [19] H. Kaki, A. Nisino, and T. Ise, "Distribution voltage control for DC microgrid with fuzzy control and gain-scheduling control," in *Proc. IEEE 8th Int. Conf. Power Electron. ECCE Asia (ICPE & ECCE)*, Jeju City, Korea, 2011, pp. 256–263.
- [20] J. A. P. Lopes, C. L. Moreira, and A. G. Madureira, "Defining control strategies for microgrids islanded operation," *IEEE Trans. Power Syst.*, vol. 21, no. 2, pp. 916–924, May 2006.
- [21] B. K. Johnson and R. H. Lasseter, "An industrial power distribution system featuring UPS properties," in *Proc. IEEE 24th Annu. Conf. Power Electron. Spec.*, Seattle, WA, USA, 1993, pp. 759–765.
- [22] B. K. Johnson, R. H. Lasseter, F. L. Alvarado, and R. Adapa, "Expandable multi-terminal DC systems based on voltage droop," *IEEE Trans. Power Del.*, vol. 8, no. 4, pp. 1926–1932, Oct. 1993.
- [23] S. Choi, M. Sin, D. Kim, and Y. Jung, "Versatile power transfer strategies of PV-battery hybrid system for residential use with energy management system," in *Proc. Int. Conf. Power Electron.*, Hiroshima, Japan, 2014, pp. 409–414.
- [24] H. Tazvinga, B. Zhu, and X. Xia, "Optimal power flow management for distributed energy resources with batteries," *Energy Convers. Manage.*, vol. 102, pp. 104–110, Sep. 2015.
- [25] S. Sivakumar and D. Devaraj, "Congestion management in deregulated power system by rescheduling of generators using generic algorithm," in *Proc. Int. Conf. Power Signals Control Comput. (EPSCICON)*, Thrissur, India, 2014, pp. 1–5.
- [26] H. Keshtkar, A. Darvishi, and S. H. Hosseini, "Analysis on reserve effects on congestion management results in an integrated energy and reserve power market," in *Proc. 19th Iranian Conf. Elect. Eng. (ICEE)*, Tehran, Iran, 2011, pp. 1–6.
- [27] T. Bhattacharjee and A. K. Chakraborty, "Congestion management in a deregulated power system using NSGAI," in *Proc. IEEE 5th Conf. Power India*, Murthal, India, 2012, pp. 1–6.
- [28] L. Chen, H. Suzuki, T. Wachi, and Y. Shimura, "Components of nodal prices for electric power systems," *IEEE Trans. Power Syst.*, vol. 17, no. 1, pp. 41–49, Feb. 2002.
- [29] Y. Okabe and K. Sakai, "QoEn (quality of energy) routing toward energy on demand service in the future Internet," *Inst. Electron. Inf. Commun. Eng. Tech. Rep.*, vol. 109, no. 262, pp. 9–12, 2009.
- [30] T. Takuno, Y. Kitamori, R. Takahashi, and T. Hikihara, "AC power routing system in home based on demand and supply utilizing distributed power sources," *Energies*, vol. 4, pp. 717–726, Apr. 2011.
- [31] R. Abe, H. Taoka, and D. McQuilkin, "Digital grid: Communicative electrical grids of the future," *IEEE Trans. Smart Grid*, vol. 2, no. 2, pp. 399–410, Jun. 2011.
- [32] T. Kato, K. Yuasa, and T. Matsuyama, "Energy on demand: Efficient and versatile energy control system for home energy management," in *Proc. SmartGridComm*, Brussels, Belgium, 2011, pp. 392–397.
- [33] T. Kato, K. Tamura, and T. Matsuyama, "Adaptive storage battery management based on the energy on demand protocol," in *Proc. SmartGridComm*, Tainan, Taiwan, 2012, pp. 43–48.



**Saher Javid** received the Bachelor's degree in computer science from Allama Iqbal Open University, Islamabad, in 2004; the Master's degree in information technology from the University of the Punjab, Lahore, Pakistan, in 2007; and the Ph.D. degree in information science from the Japan Advanced Institute of Science and Technology, in 2014. Since 2014, she has been an Assistant Professor with the Graduate School of Informatics, Kyoto University. Her research interests include distributed sensing control and energy management.



**Yuhei Kurose** received the Bachelor's degree in electrical and electronic engineering, and the Master's degree in informatics from Kyoto University, in 2013 and 2015, respectively.



**Takekazu Kato** received the B.S. and D.S. degrees from Okayama University, Japan, in 1997 and 2001, respectively. He is currently an Associate Professor with the Graduate School of Informatics, Kyoto University. His research interests include pattern recognition, computer vision, and energy management. He is a Member of the IEEE Communications Society, IPSJ, and IEICE.



**Takashi Matsuyama** received the B.Eng., M.Eng., and D.Eng. degrees in electrical engineering from Kyoto University, Japan, in 1974, 1976, and 1980, respectively. He is currently a Professor with the Department of Intelligence Science and Technology, Graduate School of Informatics, Kyoto University.

He has been studying cooperative distribute sensing-control-reasoning systems for over 30 years. Their application fields include knowledge-based image understanding, visual surveillance, 3-D video, human-computer interaction, and smart energy management. He has authored over 100 journal papers and over 20 books, including three research monographs.